Pharmacophore

ISSN-2229-5402

Journal home page: http://www.pharmacophorejournal.com

A NEW PROTON TRANSFER COMPLEX OF 2-AMINO-4,6-DIMETHOXYPYRIMIDINE WITH 2,6-DICHLORO-4-NITROPHENOL: SPECTROSCOPIC AND DFT/TD-DFT STUDIES

Maram T. Basha[1]*, Saied M. Soliman[2,3], Reem M. Alghanmi[1], Nada M. Wafi[1]

1. *Chemistry Department, Faculty of Science, University of Jeddah, Jeddah, Saudi Arabia*
2. *Department of Chemistry, Rabigh College and Art, King Abdulaziz University, Rabigh, Saudi Arabia*
3. *Department of Chemistry, Faculty of Science, Alexandria University, Ibrahimia, Alexandria, Egypt.*

ARTICLE INFO

Received:
19th Mar 2019
Received in revised form:
27th Jul 2019
Accepted:
02th Aug 2019
Available online:
21th Oct 2019

Keywords: Proton transfer, 2,6-dichloro-4-nitrophenol, pyrimidine, spectroscopy, DFT

ABSTRACT

A new proton transfer (PT) complex formed on the reaction between 2,6-dichloro-4-nitrophenol (DCNP) as a proton donor and 2-amino-4,6-dimethoxypyrimidine (ADMP) as a proton acceptor has been investigated and characterized experimentally and theoretically. The experimental work has been carried out in three different polar solvents, including methanol, ethanol, and acetonitrile as well as in the solid state. The molecular composition of the PT complex was determined employing Job's and photometric titration methods to be 1:1 in all studied solvents confirming that the complex's stoichiometry is solvent-independent. The PT formation constant (K_{PT}) and the molar extinction coefficient (ε) in the selective solvents were calculated using the modified Benesi-Hildebrand equation. The K_{PT} values are highest in the protic solvent (EtOH) and lowest in the aprotic solvent (ACN). The spectroscopic physical parameters have been determined, where the more negative ΔG° was recorded in EtOH and was in good agreement with the PT formation constant. Furthermore, a sensitive spectrophotometric method for determining ADMP is proposed and validated statistically. The solid complex was synthesized and characterized, utilizing elemental analysis, ^{1}H NMR, and FT-IR spectroscopy and they confirmed the formation of 1:1 PT complex. The optimized geometries of DCNP, ADMP, and the proton transfer DCNP-ADMP complexes were calculated using B3LYP and CAM-B3LYP methods as well as 6-31++G (d,p) basis sets. The reactivity descriptors were used to describe the electron transfer processes among the DCNP and ADMP molecules. The significant electron density of 0.142 e was transferred from ADMP to DCNP. The electronic spectra of DCNP-ADMP complex were predicted using Time-dependent density functional theory (TD-DFT) calculations and compared with the experimental data.

To Cite This Article: Basha M.T., Soliman S.M., Alghanmi R. M., Wafi N. M., (2019) .A new proton transfer complex of 2-amino-4,6-dimethoxypyrimidine with 2,6-dichloro-4-nitrophenol: spectroscopic and DFT/TD-DFT studies", ***Pharmacophore, 10(5),*** *5-22.*

Introduction

Over the past few decades, heterocyclic compounds received great attention due to their significant applications in medicinal chemistry.[1] Among these heterocyclic compounds are pyrimidines, which are aromatic organic compounds containing two nitrogen atoms with a profound presence on DNA and RNA due to their pairing with adenine and guanine. Moreover, many natural products, especially vitamins such as thiamine, uracil, and thymine, are pyrimidine derivatives.[2] These pyrimidine derivatives are also utilized as corrosion inhibitors and chelating agents[3] In addition, they exhibit extensive applications in biological and clinical fields [4, 5] including antibacterial, antifungal, antiviral, anticonvulsant, antiasthmatics, antiallergic, and anticancer properties. Therein, aminopyrimidines are used as therapeutic agents and are major components in medical formulations [6, 7] Furthermore, pyrimidine derivatives were found to be important in the pathology of Alzheimer's disease and in many Marin alkaloids that show pharmacological properties[8] Thereby, the broad range of applications of pyrimidines, and their novel derivative have motivated researchers to synthesize numerous biologically active drugs. Moreover, the ability of heterocyclic pyrimidines to form hydrogen-bonded complex via hetero ring or amino nitrogens was observed. [9]

Hydrogen bonding and proton transfer processes are fundamental in chemical and biological systems.[10-12] They play a key role in photochemistry and photobiology in acid/base complexes, as well as solute/solvent systems.[13, 14] Moreover,

Corresponding Author: Maram T. Basha; Chemistry Department, Faculty of Science, University of Jeddah, P.O. Box 80327, Jeddah 21589, Saudi Arabia. Email: mtbasha @ uj.edu.sa

these reactions were found to be essential in constructing supra-molecular structures,[15] controlling the speed of enzymatic reactions,[16] and stabilizing bio-molecular structures.[17] Proton transfer complexes of phenol, especially 2,6–dichloro–4-nitrophenol with nitrogen and oxygen bases have been investigated employing spectroscopic and theoretical studies.[9, 18-24] Considering the tremendous biological and pharmacological applications of pyrimidines and in continuation of our interest in proton transfer (PT) complexes, in this current investigation, the reaction between 2,6-dichloro-4-nitrophenol as a proton donor and 2-amino-4,6-dimethoxypyrimidine as a proton acceptor was examined in both solution and solid states. The novel complex was studied experimentally and theoretically. The main target of this study was to determine the molecular composition, formation constant, and the spectroscopic physical parameters of PT complex in different polar solvents. Furthermore, the PT solid complex was prepared and characterized by elemental analysis, ^{1}H NMR, and FT-IR spectra. The density functional theory (DFT) was also applied to study the energy optimization of the formed PT complex, atomic charge distribution, molecular electrostatic potential, as well as reactivity parameters. The electronic spectra were computed employing TD-DFT/6-31++G(d,p) method. Natural bond orbital (NBO) analysis was also considered. A significant aim of this work was to develop a better understanding of PT complex with consistency and correlation between both measured and calculated results.

Experimental

Material and stock solutions

All chemicals used were reagent grade and were used without further purification. DCNP and ADMP (purity ≥ 98%) were purchased from Sigma-Aldrich. Standard stock solutions of DCNP (1×10^{-3} mol L^{-1}) and ADMP (1×10^{-2} mol L^{-1}) were prepared immediately before each series of measurements by dissolving the appropriate amount of compound in 25 mL of each solvent. The stock solutions of proton donor and proton acceptor were stored in the dark for up to one week and monitored for stability.

Instrumentation and physical measurements

The electronic absorption spectra of the DCNP, ADMP, and the formed PT complex were measured in different solvents using the Shimadzu 1800 UV-Vis spectrophotometer (Japan) at the range of 300-600 nm connected to a Shimadzu TCC-ZUOA temperature controller unit. FT-IR spectra (KBr disks) at the range of 4000-400 cm^{-1} were used to measure the reactants and the solid PT complex and were recorded on a Perkin-Elmer model Frontier (USA). ^{1}H NMR spectrum was recorded in DMSO-*d6*, employing the Bruker AV-700 MHz spectrometers using 10 mg of the sample in dimethylsulfoxide (DMSO-*d6*) and tetramethylsilane (TMS) as an internal standard. Elemental analyses (C, H, and N) were performed on a Perkin-Elmer 2400 micro Analyzer (USA) in the microanalytical laboratory of Cairo University, Egypt.

Synthesis of the PT complex and elemental analysis

The solid PT complex of DCNP with ADMP was synthesized by adding one mmol of both reactants in 20 ml MeOH. The obtained solution was stirred for one hour and the solvent was allowed to evaporate at room temperature. The solid yellow products were filtered off, washed with MeOH, and dried over anhydrous calcium chloride in a desiccator. The yellow PT complex melted at 138 °C. The PT complex was characterized by elemental analyses and the analytical calculations for (DCNP-ADMP) $C_{12}H_{12}Cl_2N_4O_5$ (M/W: 363.15 g/mol), C, 39.69 %; H, 3.33 %; N, 15.43 %. Found: C, 39.16 %; H, 3.38 %; N, 14.93 %. Hence, the complex was formed in a 1:1 ratio (DCNP: ADMP). ^{1}H NMR (DMSO-*d6* ppm): 8.27, H(33,34); 6.63, H(13,14,35); 5.38, H(12); 3.77, H(15,16,17,18,19,20). The suggested structure of the formed PT complex is presented in **Fig. 1.**

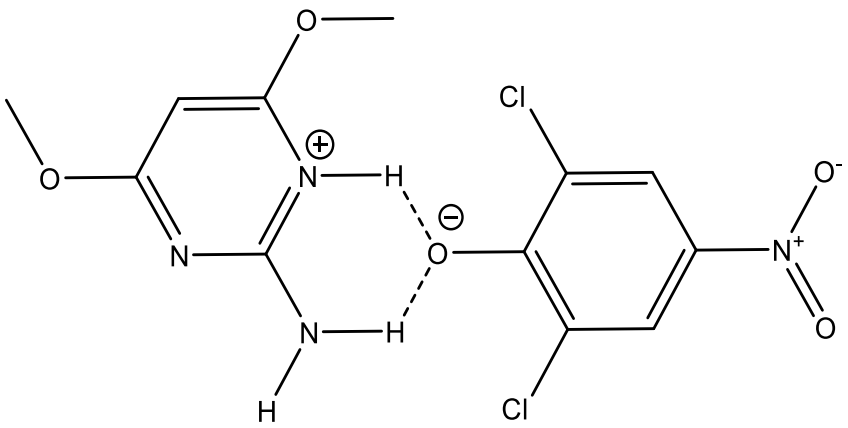

Fig.1. Suggested structure of DCNP-ADMP PT complex.

Computational details

The free dichloro-4-nitrophenol (DCNP), 2-amino-4,6-dimethoxypyrimidine (ADMP), and DCNP-ADMP PT complex were calculated using Gaussian 09 software [25] while Gauss View 4.1 and Chemcraft programs [26, 27] were used for

visualization purposes. For this task, the B3LYP and CAM-B3LYP methods combined with 6-31++G (d,p) were used. The atomic charges were predicted using the natural bond orbital (NBO) method.[28, 29] The UV–Vis spectra were simulated using the time-dependent density TD-DFT method considering the solvent (EtOH) effects, using the polarizable continuum model (PCM). [30]

Results and Discussion

Observation of the PT band

The UV-Visible absorption spectra of the proton donor DCNP, proton acceptor ADMP, and their PT complex in MeOH, EtOH, and ACN were recorded as illustrated in **Fig. 2**. Sharp absorption bands were observed at the range of 395- 424 nm in the investigated solvents (**Fig. 2**), confirming the $\pi \rightarrow \pi^*$ transition in the formed PT complex. These absorption bands are associated with a change in color of the solution, where deep yellow color was observed upon mixing of the reactants in all solvents. The PT complex absorption bands appeared at 424, 406, and 395 nm in ACN, EtOH, and MeOH, respectively, demonstrating the high sensitivity of the PT reaction to various solvents. Notably, the absorption of the complex in all solvents stabilizes after two hours (**Fig. 3**). Thus, the PT solutions were kept in the dark for two hours to ensure complete complex formation. The spectral measurements were recorded using a blank solution that had the same concentration of the proton donor DCNP in order to eliminate any interference between the complex and proton donor bands. The absorbance of the PT complex was found to increase with increasing proton acceptor concentration (ADMP) as shown in **Table 1**, supporting the proton transfer interaction that is stabilized by hydrogen bonds. Good evidence of this conclusion is that the DCNP has strong acidic properties (pK_a =3.55),[9, 31] and the ADMP has strong basic properties.

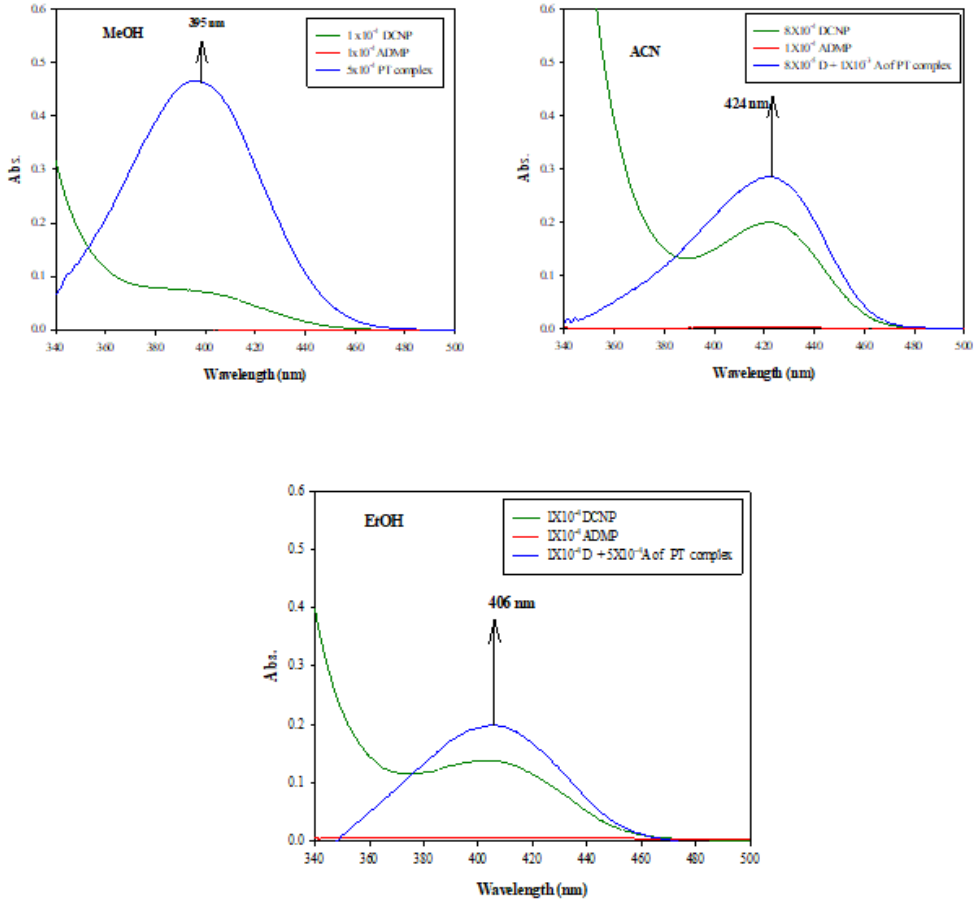

Fig. 2. Electronic spectra of (DCNP) mol·L^{-1}, (ADMP) mol·L^{-1}, and PT complex in different solvents.

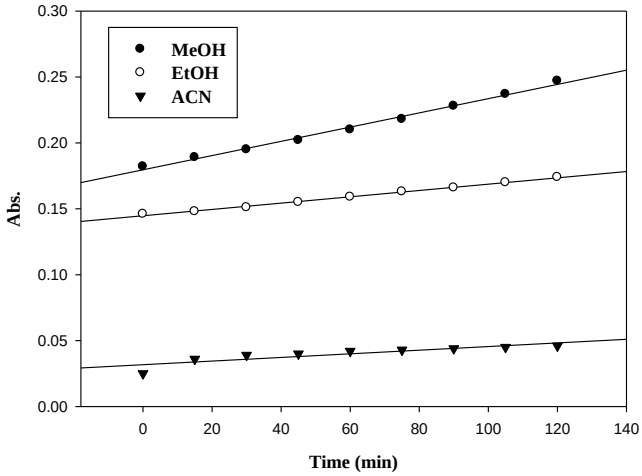

Fig. 3. Effect of time on the [DCNP-ADMP] PT complex in different solvents.

Molecular composition of the PT complex

The molecular composition of the PT complex was estimated, employing Job's method of continuous variations and spectrophotometric titration method.[32, 33] The obtained results from Job's method display the maximum absorbance at a 0.5-mole fraction, indicating a 1:1 (donor: acceptor) stoichiometry for the PT complex (**Fig. 4**). Moreover, the spectrophotometric titration method confirmed this stoichiometry, where two straight lines are produced intercepting at an A/D ratio equal to one (**Fig. 5**). Indeed, the obtained results reflect that the polarity of the solvent did not affect the molecular composition of PT complex.

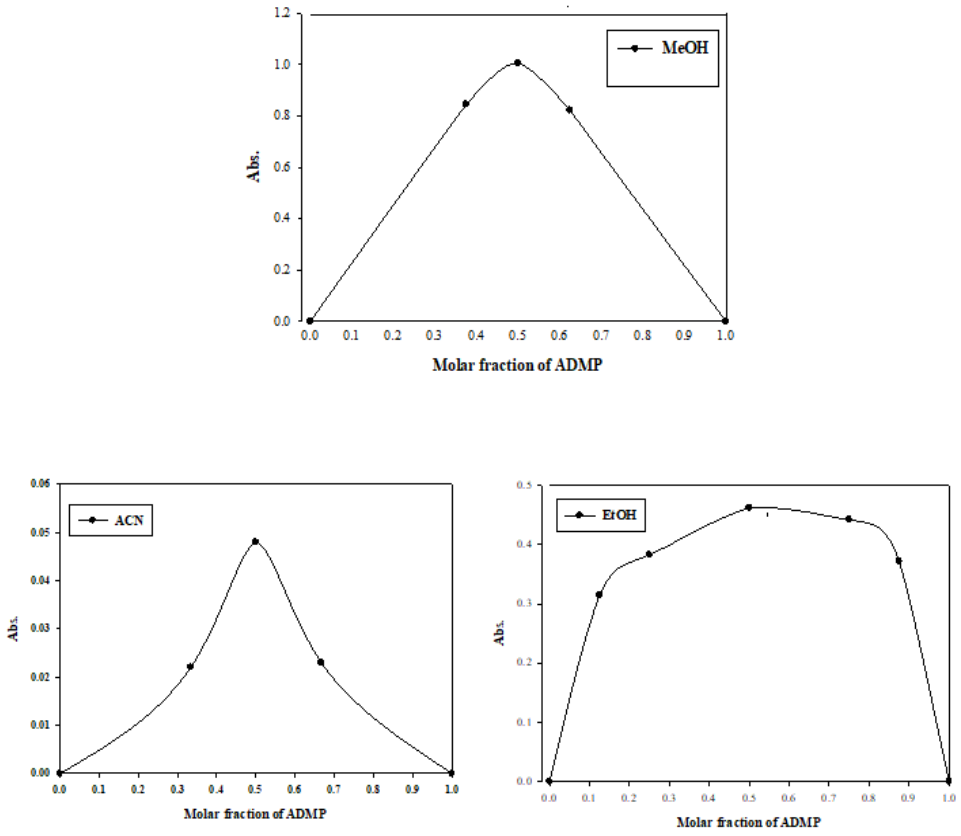

Fig. 4. Job's method plots of [DCNP-ADMP] PT complex in different solvents.

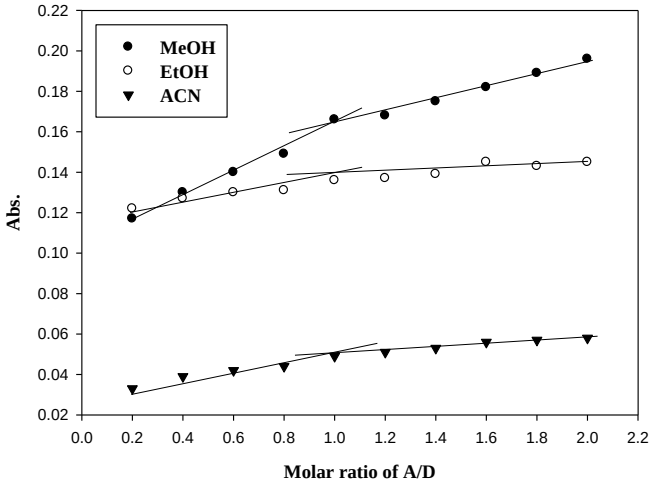

Fig. 5. Spectrophotometric titration plots of the [DCNP-ADMP] PT complex in different solvents.

Formation constant of PT reaction

The modified Benesi-Hildebrand equation [34] under the condition [A] > [D], Eq. (1) was applied to calculate the PT formation constant (K_{PT}) and the molar extinction coefficient (ε) in different solvents, based on the spectral data illustrated in **Table 1**.

$$C_D^o C_A^o / A = 1/ K_{PT}\varepsilon + (C_D^o + C_A^o)/\varepsilon \quad (1)$$

where C_D^o and C_A^o are the concentrations of DCNP and ADMP, respectively, and *A* is the absorbance of the PT-band. Plotting the values $C_D^o C_A^o / A$ against $(C_D^o + C_A^o)$, straight lines were obtained supporting the formation of a 1:1 complex in all solvents (**Fig. 6**). The slope and intercept were equal to 1/ε and 1/K_{PT}ε, respectively. The values of K_{PT} and ε are reported in **Table 2**, and indicate that the formed complex was of high stability in all of the solvents investigated. The highest value of the PT formation constant is in EtOH compared to MeOH or can, which could be correlated to hydrogen bond donor (α), hydrogen bond acceptor (β), and dipolarity/polarizability (Π*) parameters of solvents.[35] Interestingly, EtOH has near values of both α and β, resulting in hydrogen bond formation between EtOH and DCNP and ADMP moieties of the complex, stabilizing the ground state of the PT complex, increasing the K_{PT} to 2×10^3 L mol^{-1}. On the other hand, the least value of K_{PT} was observed in an aprotic solvent, ACN, that could be explained depending on its high Π*value, which led to self-association, producing a dimer of ACN molecules. [35] These properties result in increasing the steric hindrance and decreasing effective dipole moment, obstructing the PT process that reduces the K_{PT} to 250 L mol^{-1}, as shown in **Table 2**. Collectively, the results indicate that polarity is the key factor in the increase of K_{PT} with decreasing electric permittivity of the solvent. Additionally, the formation of intermolecular hydrogen bonding between protic solvents with ADMP could lead to high K_{PT} in EtOH and MeOH compared to that of CAN.[11, 12]

Table 1. Bensi-Hildebrand data of [DCNP-ADMP] PT complexes in different solvents.

Solvents	C^o_D	C^o_A	Abs.	$C^o_D C^o_A$ /A	$C^o_D + C^o_A$	R^2
MeOH	6.0×10^{-4}	1.0×10^{-4}	0.159	3.77×10^{-7}	7.0×10^{-3}	0.9941
	8.0×10^{-4}	1.0×10^{-4}	0.196	4.08×10^{-7}	9.0×10^{-3}	
	1.0×10^{-3}	1.0×10^{-4}	0.223	4.48×10^{-7}	1.1×10^{-3}	
	1.4×10^{-3}	1.0×10^{-4}	0.251	5.58×10^{-7}	1.5×10^{-3}	
	1.8×10^{-3}	1.0×10^{-4}	0.297	6.06×10^{-7}	1.9×10^{-3}	
	2.0×10^{-3}	1.0×10^{-4}	0.304	6.58×10^{-7}	2.1×10^{-3}	
	2.4×10^{-3}	1.0×10^{-4}	0.323	7.43×10^{-7}	2.5×10^{-3}	
	2.8×10^{-3}	1.0×10^{-4}	0.350	8.00×10^{-7}	2.9×10^{-3}	
	3.2×10^{-3}	1.0×10^{-4}	0.367	8.72×10^{-7}	3.3×10^{-3}	
	3.6×10^{-3}	1.0×10^{-4}	0.392	9.18×10^{-7}	3.7×10^{-3}	
	4.0×10^{-3}	1.0×10^{-4}	0.402	9.95×10^{-7}	4.1×10^{-3}	

EtOH	4.0×10^{-4}	1.0×10^{-4}	0.055	7.27×10^{-7}	5.0×10^{-3}	0.9974
	6.0×10^{-4}	1.0×10^{-4}	0.060	1.00×10^{-6}	7.0×10^{-3}	
	1.2×10^{-3}	1.0×10^{-4}	0.078	1.54×10^{-6}	1.3×10^{-3}	
	2.0×10^{-3}	1.0×10^{-4}	0.091	2.20×10^{-6}	2.1×10^{-3}	
	2.4×10^{-3}	1.0×10^{-4}	0.098	2.45×10^{-6}	2.5×10^{-3}	
	3.2×10^{-3}	1.0×10^{-4}	0.105	3.05×10^{-6}	3.3×10^{-3}	
	4.4×10^{-3}	1.0×10^{-4}	0.107	4.11×10^{-6}	4.5×10^{-3}	
ACN	4.0×10^{-4}	8.0×10^{-4}	0.030	1.07×10^{-5}	1.2×10^{-3}	0.9955
	1.0×10^{-3}	8.0×10^{-4}	0.067	1.19×10^{-5}	1.8×10^{-3}	
	3.2×10^{-3}	8.0×10^{-4}	0.153	1.67×10^{-5}	4.0×10^{-3}	
	4.0×10^{-3}	8.0×10^{-4}	0.182	1.76×10^{-5}	4.8×10^{-3}	
	4.8×10^{-3}	8.0×10^{-4}	0.194	1.98×10^{-5}	5.6×10^{-3}	
	5.6×10^{-3}	8.0×10^{-4}	0.214	2.09×10^{-5}	6.4×10^{-3}	

Table 2. Solvent parameters, wavelength, formation constant (K_{PT}), and molar extinction coefficient (ε) of [DCNP-ADMP] PT complexes in different solvents.

Solvents	α	β	Π*	λ_{max} nm	K_{PT} L mol^{-1}	ε L mol^{-1} cm^{-1}
MeOH	0.98	0.62	0.60	395	667	5000
EtOH	0.83	0.77	0.54	406	2000	1250
ACN	0.19	0.31	0.75	424	250	500

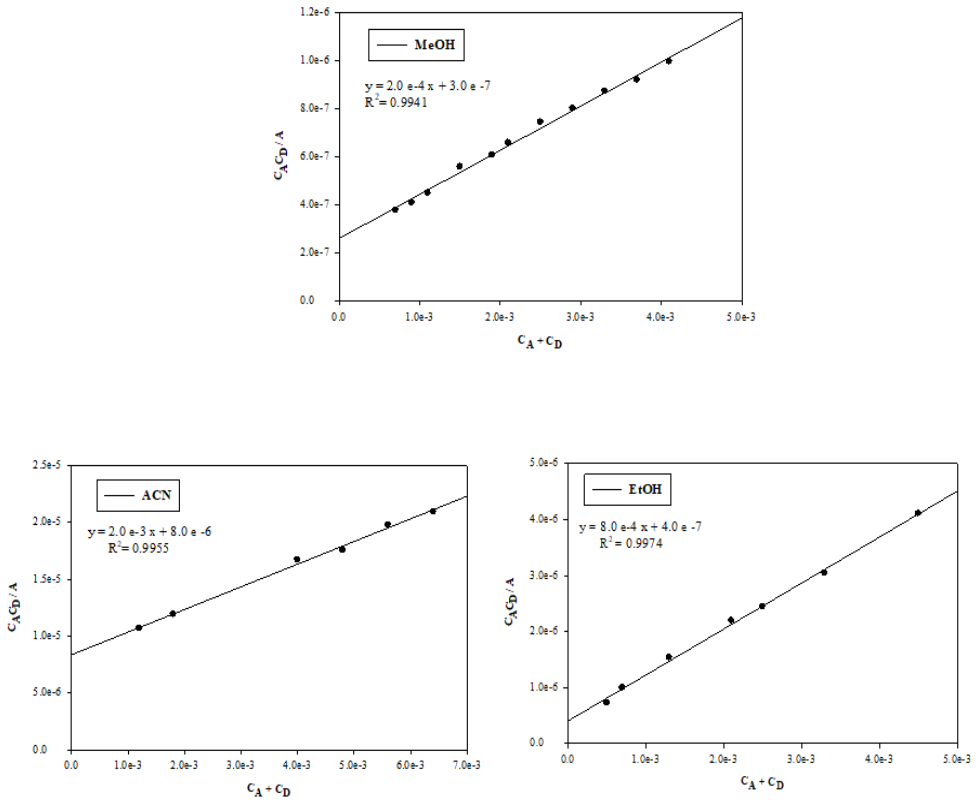

Fig. 6. Bensie-Hildebrand plots of 1:1[DCNP-ADMP] PT complex in different solvents.

Determination of the spectroscopic physical parameters

The transition dipole moment (μ),[36] which is the essential parameter indicating the presence of proton transfer interactions, and the oscillator strength (*f*),[37] which is the dimensionless quantity, were calculated in the investigated solvents by applying the following equations;

$$\mu = 0.0958\left[\varepsilon_{max} \cdot \Delta\nu_{1/2} / \bar{\nu}_{max}\right]^{1/2} \quad (2)$$

$$f = 4.32\times10^{-9}\left[\varepsilon_{max} \cdot \Delta\nu_{1/2}\right] \quad (3)$$

where $\Delta\nu_{1/2}$ is the half bandwidth of the absorbance, ε_{max} and $\bar{\nu}_{max}$ are the molar extinction coefficient and wavenumber at the maximum absorption peak of the PT complex, respectively. The results are listed in **Table 3** and show that the values of both the transition dipole moment and the oscillator strength were relatively high, proving the high possibility of proton transfer from DCNP to ADMP, in addition to the high stability of PT complex in all solvents. This stability was further supported by calculating the standard free energy changes of the formed complexes (ΔG°) [38] using the following equation;

$$\Delta G^{o} = -2.303RT\log K_{PT} \quad (4)$$

Where ΔG° is the free energy of PT complexes (kJ mol^{-1}), *R* is the gas constant (8.314 J mol^{-1} K^{-1}), *T* is the absolute temperature in Kelvin, and K_{PT} is the formation constant of PT complexes in different solvents at room temperature (25°C). The obtained results indicate that the ΔG° had negative values in all solvents, as compiled in **Table 3**, confirming the spontaneous reaction of PT complexes. Clearly, the values of ΔG° aligned with the formation constant values, where the more negative ΔG° recorded was in EtOH (– 18.84 kJ mol^{-1}) and the bond between the donor and acceptor becomes stronger (higher K_{PT}).

Table 3. The spectroscopic physical and thermodynamic parameters.

Solvents	λ_{max} nm	*f*	μ (Debye)	$-\Delta G°$ (kJ mol^{-1})
MeOH	395	0.133	3.35	16.12
EtOH	406	0.029	1.59	18.84
ACN	424	0.051	2.16	13.69

Application of the studied PT reaction

- **Optimization of reaction temperature**

The effect of temperature on the formation of PT complex was studied by following the absorbance of PT complexes resulted by mixing (1×10^{-4} or 8×10^{-4} mol L^{-1}) DCNP with different concentrations of ADMP in different solvents and across the temperature range of 20 – 40°C, as displayed in **Table 4.** We can observe from **Table 4** that the absorbance slightly decreases with increasing temperature and 20°C was the optimum temperature where the absorbance recorded the highest value in all solvents.

Table 4. Effect of temperature on [DCNP-ADMP] PT complexes in different solvents.

Solvents	[DCNP] mol L^{-1}	[ADMP] mol L^{-1}	Abs. at λ_{max} = 395 nm				
			20 °C	**25 °C**	**30 °C**	**35 °C**	**40 °C**
MeOH	1×10^{-4}	8.0×10^{-4}	0.280	0.252	0.230	0.210	0.192
	1×10^{-4}	1.4×10^{-3}	0.362	0.335	0.310	0.287	0.265
	1×10^{-4}	1.8×10^{-3}	0.381	0.348	0.321	0.296	0.273
	1×10^{-4}	2.8×10^{-3}	0.406	0.371	0.339	0.311	0.287
	1×10^{-4}	3.2×10^{-3}	0.430	0.397	0.365	0.337	0.312
	1×10^{-4}	3.6×10^{-3}	0.462	0.426	0.393	0.364	0.338
	1×10^{-4}	4.0×10^{-3}	0.487	0.450	0.417	0.387	0.361
EtOH	[DCNP] mol L^{-1}	[ADMP] mol L^{-1}	Abs. at λ_{max} = 406 nm				
			20 °C	**25 °C**	**30 °C**	**35 °C**	**40 °C**
	1×10^{-4}	4.0×10^{-4}	0.042	0.047	0.042	0.041	0.041
	1×10^{-4}	6×10^{-4}	0.058	0.059	0.058	0.057	0.057
	1×10^{-4}	1.6×10^{-3}	0.074	0.072	0.069	0.067	0.065
	1×10^{-4}	2.4×10^{-3}	0.085	0.085	0.081	0.078	0.075
	1×10^{-4}	2.8×10^{-3}	0.090	0.089	0.086	0.082	0.079
	1×10^{-4}	4.8×10^{-3}	0.123	0.120	0.114	0.108	0.104

	1×10^{-4}	5.2×10^{-3}	0.131	0.127	0.120	0.115	0.109
ACN	[DCNP] mol L^{-1}	[ADMP] mol L^{-1}	Abs. at λ_{max} = 424 nm				
			20 °C	**25 °C**	**30 °C**	**35 °C**	**40 °C**
	8×10^{-4}	4.0×10^{-4}	0.110	0.107	0.102	0.098	0.096
	8×10^{-4}	1.0×10^{-3}	0.155	0.152	0.148	0.143	0.140
	8×10^{-4}	1.8×10^{-3}	0.189	0.185	0.181	0.176	0.173
	8×10^{-4}	2.8×10^{-3}	0.215	0.212	0.207	0.202	0.199
	8×10^{-4}	4.4×10^{-3}	0.263	0.258	0.253	0.246	0.241
	8×10^{-4}	5.6×10^{-3}	0.338	0.333	0.325	0.316	0.308

- **Analytical data**

For the determination of ADMP, a new spectrophotometric method was proposed, which is simple, rapid, and accurate based on the formation of 1:1 [DCNP-ADMP] PT complex. Therefore, under the optimized experimental condition, Beer's plots at different 1:1 molar ratios between DCNP and ADMP in different solvents were produced. The regression equation of the lines in the investigated solvents was derived, utilizing the least-squares method. The plots were linear, with good correlation coefficient and small intercepts that had small values of confidence intervals over the concentration ranges of 6.21–43.44, 6.21–62.06, and 15.52–232.73 µg ml^{-1} in EtOH, MeOH, and ACN, respectively (**Table 5)**. The limit of detection (LOD) and limit of quantification (LOQ) were calculated [39] and their small values confirmed the high sensitivity of the proposed method in protic solvents (**Table 5**). Furthermore, the evaluation of accuracy and precision of the method was achieved by analyzing solutions containing five different amounts of ADMP (within the linear range) and measuring the absorbance of PT complexes with DCNP in all studied solvents. Additionally, the recovery percentage, the standard deviation (S), and relative standard deviation (%RSD) were calculated, as presented in **Table 6**. It was found that the recovery percentage had values close to 100 % with % RSD ranging from 0.83 to 2.03 %, indicating that the proposed method is accurate and precise. The difference between the mean and true value [39] was significant, which could be due to the indeterminate error $\pm \frac{t_{n-1}S}{\sqrt{n}}$ (**Table 6**).

Table 5. Quantification parameters of [DCNP-ADMP] PT complexes in different solvents.
*y = bx + a, where y is the absorbance and x is the ADMP concentration in µg ml^{-1}.

Parameters	Solvents		
	MeOH	EtOH	ACN
Beer's law limits, µg ml^{-1}	6.21 – 62.06	6.21 – 43.44	15.52 – 232.73
Limit of detection, µg ml^{-1}	2.72	7.82	26.65
Limit of quantification, µg ml^{-1}	9.08	26.05	88.85
Regression equation*	y = 0.0082x + 0.0235	y = 0.0026x + 0.1324	y = 0.0007x + 0.0064
Intercept (a)	0.0235	0.1324	0.0064
Slope (b)	0.0082	0.0026	0.0007
Confidence interval of intercept, α	5.09×10^{-3}	5.73×10^{-3}	4.31×10^{-3}
Confidence interval of slope, β	1.32×10^{-4}	2.06×10^{-4}	2.92×10^{-5}
Correlation coefficient, r^2	0.9980	0.9695	0.9976

Table 6. Accuracy and precision of the proposed spectrophotometric method.

Solvents	Amount taken µg mL^{-1}	Amount found µg mL^{-1}	Rec, %	$\overline{X}$	S[a]	%RSD [b]	$\lvert\overline{X} - \mu\rvert$	Confidence limits [c]
	15.52	15.06	97.07	100.7	2.04	2.03	0.70	100.70 ± 2.53
	40.34	41.16	102.0					
MeOH	46.55	47.26	101.5					
	52.75	53.48	101.4					
	58.96	59.82	101.5					
	9.310	9.460	101.6	100.9	1.27	1.26	0.90	100.9 ± 1.58
	15.52	15.62	100.6					
EtOH	27.93	28.69	102.7					

	34.13	34.07	99.84					
	40.33	40.23	99.73					
	62.06	63.00	101.5					
	93.09	93.00	99.90					
ACN	139.6	141.6	101.4	101.3	0.84	0.83	1.3	101.3 ± 1.04
	170.7	174.4	102.2					
	201.7	204.4	101.4					

[a]S = standard deviation, [b] %RSD = relative standard deviation.

[c] $\overline{X} \pm \frac{t_{n-1}S}{\sqrt{n}}$,t_{n-1}= 2.77 for n = 5 at 95% confidence level.

Characterization of the isolated PT complex

- **^{1}H NMR spectra**

The ^{1}H NMR spectra of the formed 1:1 PT complex was carried out in DMSO-d_6 and presented in **Figs. 7** and **S1**. The reactant protons are observed in the complex spectrum, except the OH proton, indicating complex formation. Hence, the phenolic proton of DCNP at δ = 10.11 [20, 21] was absent in the complex spectrum (**Fig. 7**), confirming its migration toward ADMP, forming the proton transfer complex. It was also observed from **Fig 7** that the singlet peak at δ = 8.27 ppm was assigned to the symmetric protons of DCNP in the PT complex, which was similar to the observation reported in the literature.[22] The singlet resonance signal appeared at δ = 5.38 ppm and is attributed to the C (1) proton of ADMP. In addition, a sharp band appeared at about δ = 3.77 ppm is assigned to six protons of the two methoxy groups of ADMP in the PT complex. It is worth mentioning that the appearance of the broadband at δ = 6.63 ppm is attributed to two amino group proton and one NH^+ proton, confirming the involvement of the amino group and ring nitrogen of the proton acceptor ADMP in the hydrogen bonding proton transfer reaction with DCNP (**Fig. 1**).

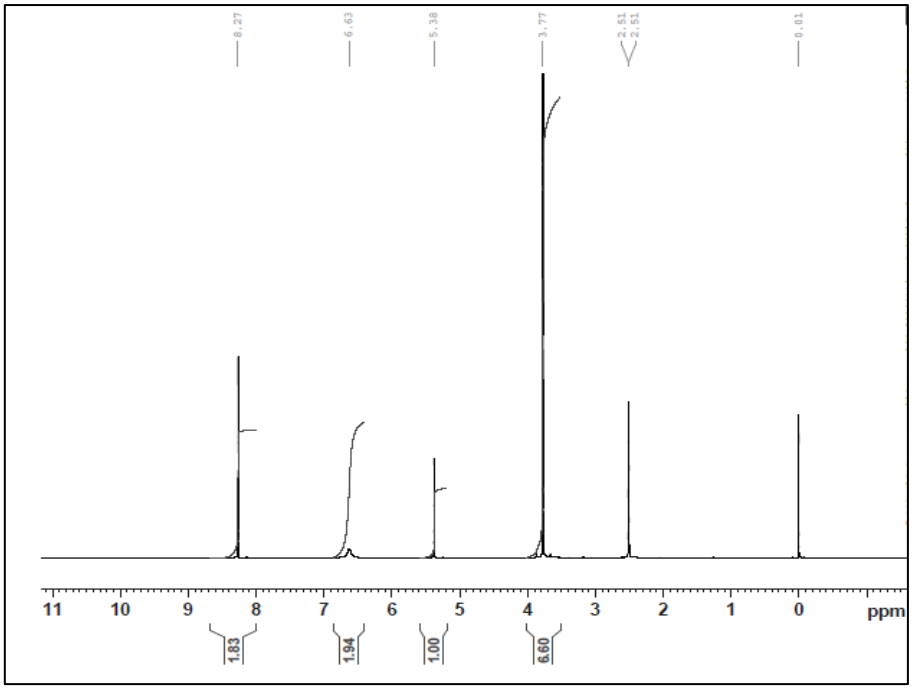

Fig. 7 ^{1}H NMR spectrum of [DCNP-ADMP] PT complex in DMSO-d_6.

- **FT-IR spectra**

The infrared spectra of the proton donor, the proton acceptor, and their 1:1 PT complex are shown in **Fig. 8** and their FT-IR bands have been summarized in **Table 7**. There were shifts on vibrational frequencies in the spectrum of PT complex compared to the reactants due to the change in electronic distributions upon complexation. On the other hand, all the infrared bands of the reactants were apparent in the complex spectrum, confirming the complex formation. The symmetric and asymmetric stretching vibrations of the $\nu^s(NH_2)$ and $\nu^{as}(NH_2)$ are broadened and shifted to the lower frequency at 3142 and 3383 cm^{-1} compared to 3309 and 3407 cm^{-1} in the spectrum of free ADMP. In addition, the shifts in plan δ (NH_2) and out of plan γ (NH_2) bending vibrations of the amino group at 1669 and 796 cm^{-1} compared to 1634 and 791 cm^{-1} of ADMP confirm the formation of PT complex. These observations strongly confirm that the amino group participates in hydrogen bonding with DCNP through oxygen phenol as presented in the proposed structure (**Fig. 1**). Moreover, the stretching vibrations of the aromatic and aliphatic ν(C–H) cannot be observed due to the overlapping of amino group stretching

vibrations. Interestingly, the complex spectrum shows a new broad absorption band at 2572 cm^{-1} due to the involvement of nitrogen pyrimidine ring in the formed proton transfer hydrogen bonding (O…H–N) (**Fig. 1**). A similar broad band at 2582 cm^{-1} is observed in FTIR spectra of 2-amino-4-methylpyridine with 2,6-dichloro-4-nitrophenol.[21] Further evidence of the formation of the PT complex is the conspicuous in the absence of the ν(OH) of DCNP at 3376 cm^{-1} in the complex spectrum due to the proton migration of phenolic proton toward the ring nitrogen of ADMP, which is in agreement with ^{1}H NMR spectrum and as reported in literature.[20-22] The ν(C=C), ν(C=N), and ν(C–N) vibrational frequencies appeared at 1574, 1444, and 1359 cm^{-1} in the spectrum of free ADMP (**Fig. 8**) compared to 1640, 1470, and 1338 cm^{-1} in the complex spectrum, respectively, supporting the PT complex formation. It was also observed in **Fig. 8** the shifts of the asymmetric and symmetric stretching vibrations of the nitro group from 1577 and 1324 cm^{-1} in the proton donor spectrum DCNP to 1558 and 1393 cm^{-1} in the complex spectrum, respectively. Furthermore, the stretching vibrations of ν(C–Cl) are shifted to 828 and 885 cm^{-1} compared to 809 and 897 cm^{-1} for free DCNP. These shifts suggest the formation of a newly 1:1 PT complex [DCNP-ADMP]. Clearly, the infrared spectra indicated the involvement of both the ring nitrogen and the amino group of ADMP in hydrogen bonding with phenolic OH of DCNP, forming the hydrogen-bonded proton transfer complex in full agreement with ^{1}H NMR results. Thus, the suggested mechanism of the formed complex is illustrated in **Scheme S1** (Supplementary data).

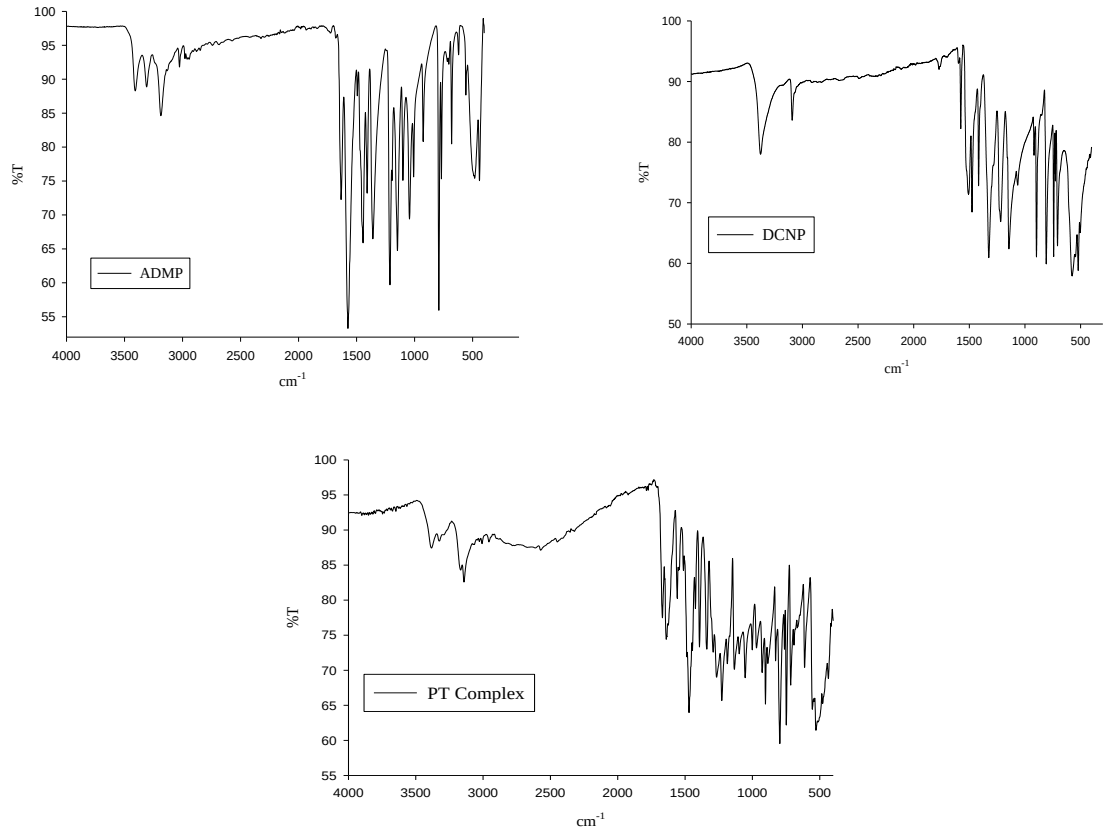

Fig. 8. FT-IR spectra of (a) ADMP; (b) DCNP; (C) [DCNP-ADMP] PT complex at the range of 4000-400 cm^{-1}.

DFT studies

There are two possible sites for the proton transfer from DCNP to ADMP: the amino group (case **A**) and the pyrimidine (case **B**) N-atoms. The results of the energy analysis, shown in **Table 8**, favored the second option either in the gas phase or in solution. The [DCNP-ADMP] PT complex with a protonated pyrimidine N-site has lower energy by 3.47, 6.75, and 6.71 kcal mol^{-1} compared to the [DCNP-ADMP] PT complex with a protonated amino group in gas, ACN, and EtOH as a solvent, respectively. The optimized molecular structures of the free DCNP, ADMP, and [DCNP-ADMP] PT complex as well as the most important bond distances are shown in **Fig. 9**. It is clear that all distances are generally longer in the PT complex when compared with the isolated DCNP and ADMP molecules. The only two exceptions from this observation are the C-N(amino) and C-O bonds of the ADMP and DCNP, respectively of the PT complex. The [DCNP-ADMP] PT complex is stabilized by two N-H…O hydrogen bonds between the O-atom of the C-O bond in the DCNP and the N-H bonds of the amino group and the protonated pyrimidine nitrogen atom. The H…O hydrogen bond distances are found to be longer (1.804 Å) in the former compared to the latter (1.586 Å) in the gas phase. The same observations were detected in solutions of the [DCNP-ADMP] complex in CAN and EtOH, but the H…O distances tend to be longer than those in the gas phase. In contrast, the N-H (amino) and N-H (pyrimidine) are shorter in the solution compared to those in the gas phase.

Table 7. Infrared wavenumbers (cm^{-1}) and band assignments for ADMP, DCNP, and [DCNP-ADMP] PT complex.

ADMP	[DCNP-ADMP]	Assignments
3407	-	$\nu^{as}(NH_2)$
-	3383	$\nu^{as}(NH_2)$+ ν(C-H) arom.
3309	-	$\nu^{s}(NH_2)$
-	3142	$\nu^{s}(NH_2)$+ ν(C-H) arom.
3186	-	ν(C-H) aliph.
	2572	O…HN hydrogen bond
2943	-	ν(C-H) aliph.
1634	1669	$\delta(NH_2)$
1574	1640	ν(C=C)
1444	1470	ν(C=N)
1359	1338	ν(C-N)
791	796	γ (NH_2)
DCNP	[DCNP-ADMP]	Assignments
3376	-	ν (O-H)
1577	1558	ν^{as} (NO_2)
1324	1393	ν^{s} (NO_2)
1144	1134	ν (C-O)
897	885	ν (C-Cl)
809	828	ν (C-Cl)

Table 8. Energetic of DCNP, ADMP, and the possible [DCNP-ADMP] PT complexes.

	B3LYP			**CAM-B3LYP**		
	Gas	ACN	EtOH	gas	ACN	EtOH
			DCNP			
E	-1431.1855	-1431.1955	-1431.1953	-1430.9644	-1430.9745	-1430.9742
ZPVE	0.0879	0.0878	0.0878	0.0896	0.0894	0.0894
$\mathbf{E_{tot}}$	-1431.0976	-1431.1078	-1431.1075	-1430.8748	-1430.8851	-1430.8848
			ADMP			
E	-548.8058	-548.8176	-548.8173	-548.5564	-548.5684	-548.5681
ZPVE	0.1591	0.1587	0.1587	0.1611	0.1607	0.1607
$\mathbf{E_{tot}}$	-548.6467	-548.6588	-548.6586	-548.3953	-548.4077	-548.4074
	Case A		**DCNP-ADMP**			
E	-1980.0001	-1980.0196	-1980.0192	-1979.5310	-1979.5508	-1979.5503
ZPVE	0.2487	0.2480	0.2480	0.2525	0.2518	0.2518
$\mathbf{E_{tot}}$	-1979.7513	-1979.7716	-1979.7711	-1979.2785	-1979.2990	-1979.2986
	Case B					
E	-1980.0050	-1980.0303	-1980.0298	-1979.5366	-1979.5606	-1979.5601
ZPVE	0.2481	0.2479	0.2479	0.2517	0.2514	0.2514
$\mathbf{E_{tot}}$	-1979.7569	-1979.7823	-1979.7818	-1979.2848	-1979.3092	-1979.3087
ΔE	3.47	6.75	6.71	3.99	6.40	6.38

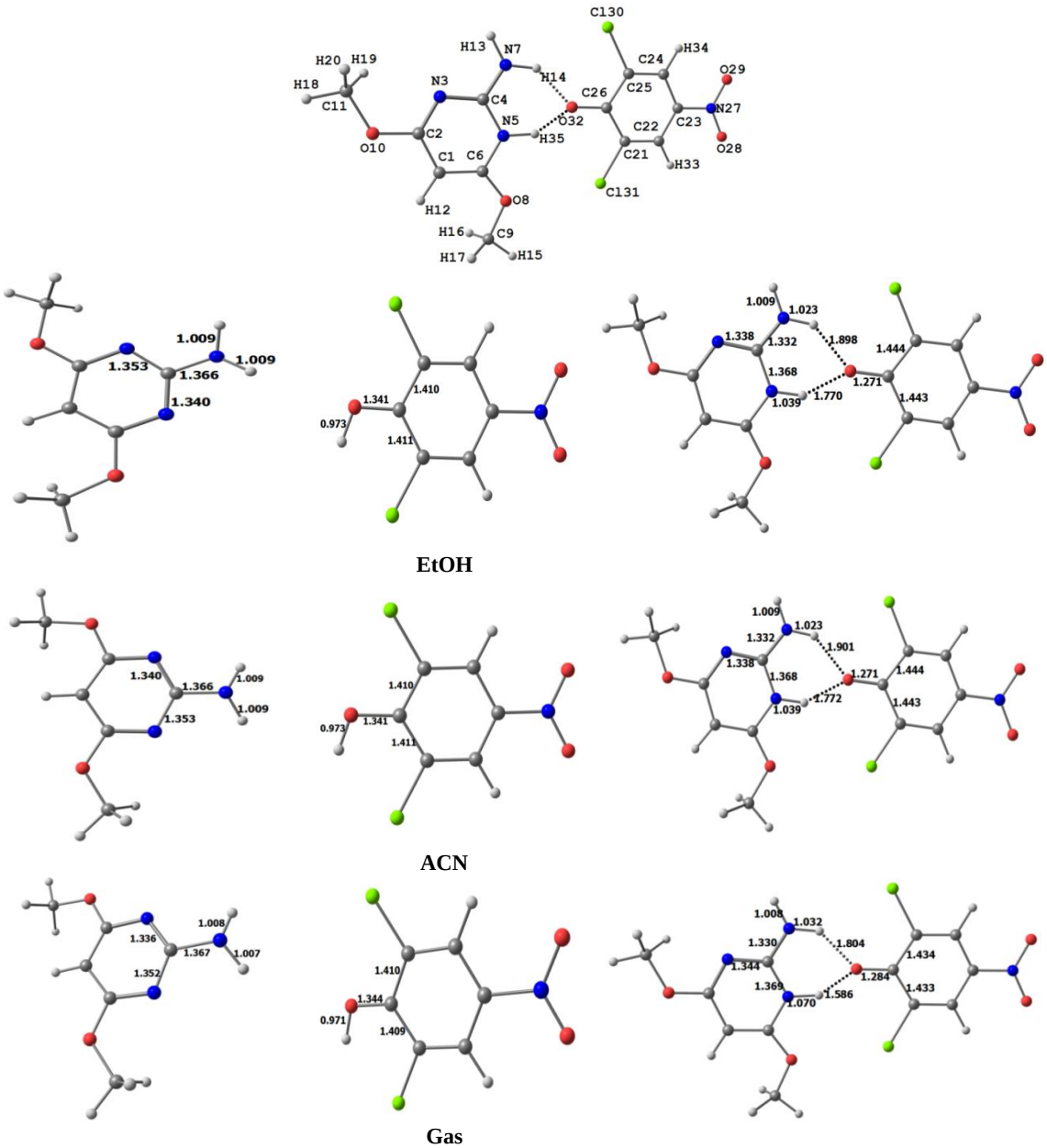

Fig. 9. The atom numbering and optimized structures of ADMP, DCNP, and [DCNP-ADMP] PT complex in the gas phase and in the solution of compounds in EtOH and ACN, using B3LYP method, similar results were obtained in case of CAM-B3LYP method. The most important interatomic distances (Å) are given.

- **Atomic charge population**

The atomic charges of the sites included in the interactions between ADMP and DCNP showed some variations compared to the [DCNP-ADMP] PT complex (**Fig. 10**). It is clear that most of the C, N, and H sites of the protonated ADMP moiety showed higher positive charge density compared to the free one. The largest variations occurred at the amino group's N atom, one of its hydrogen atoms, which is involved in the hydrogen bonding interaction with DCNP and the carbon atom bonded to the amino group. In contrast, the deprotonated DCNP showed an oxygen atom with a higher negative charge density compared to the free one. The deprotonated DCNP moiety and the protonated ADMP fragment have a net charge of –0.858 and 0.858 e, respectively. It is clear that a significant charge transfer (0.142 e) from ADMP to DCNP was noticed. Hence, the former acts as an electron donor while the latter molecule is the electron acceptor. The corresponding value in ACN as the solvent is 0.083 e. As a result, the solvent decreases the possibility of the charge transfer from ADMP to DCNP. A similar observation is noted in EtOH as the solvent.

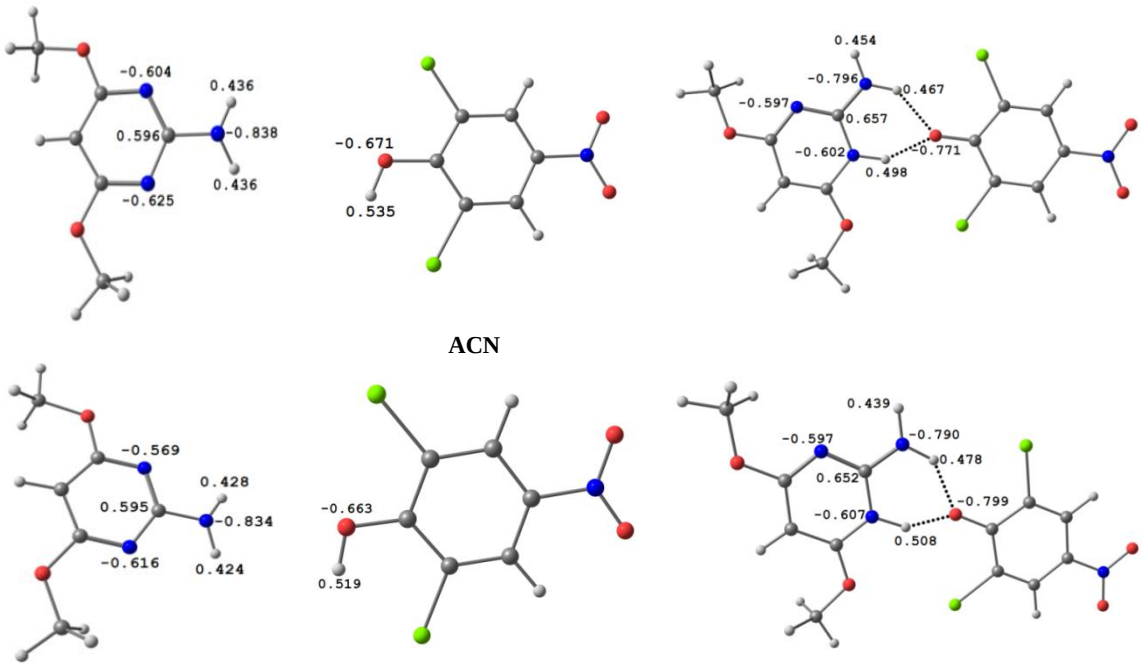

Fig. 10. Natural charges at the most important sites of ADMP, DCNP, and [DCNP-ADMP] PT complex in the gas phase and in the solution of compounds in ACN.

- **Molecular electrostatic potential (MEP) map**

The MEP maps of ADMP and DCNP are presented in **Fig. 11**. The blue region around the OH in the free DCNP indicated that this site is the best candidate to act as a proton donor site. In contrast, the MEP of ADMP showed a red region around the ring N-atom, which is considered as a good H-acceptor site.

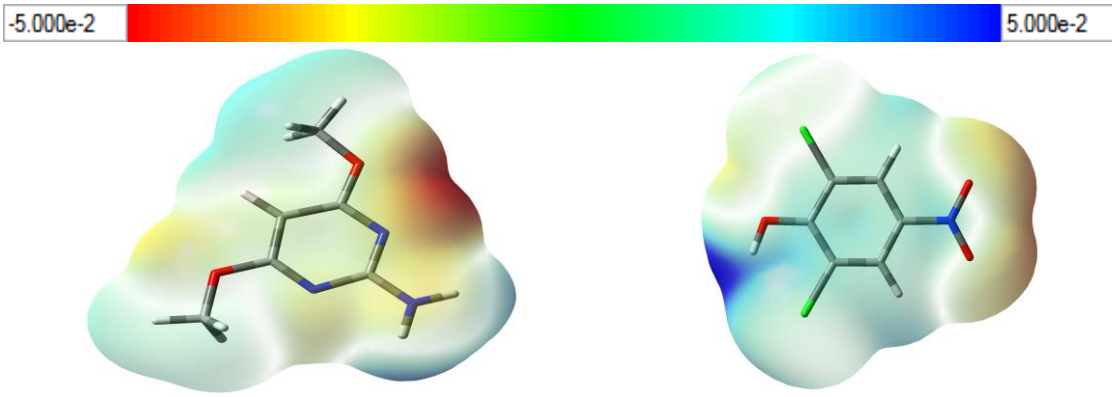

Fig. 11. The MEP maps of ADMP and DCNP molecules.

- **Reactivity studies**

The ionization potential (I), electron affinity (A), chemical potential (μ), hardness (η), and electrophilicity index (ω) [40-46] were used to understand the reaction between ADMP and DCNP molecules (Equations 5-9).

$I = -E_{HOMO}$ (5)

$A = -E_{LUMO}$ (6)

$\eta = (I-A)/2$ (7)

$\mu = -(I + A)/2$ (8)

$\omega = \mu^2/2\eta$ (9)

The results summarized in **Table 9** could shed light on the electronic properties of DCNP and ADMP. Based on the energies of the HOMO and LUMO levels of both compounds, the DCNP is the electron acceptor as indicated by the lower energy of its LUMO level compared to ADMP. In contrast, the ADMP is the electron donor because this molecule has a higher energy HOMO level than DCNP. In addition, ADMP has higher chemical potential (μ) than DCNP. As a result, the electron flow

could occur from ADMP to DCNP. In agreement with these conclusions, the electrophilicity index (ω) of DCNP is higher than that for ADMP. All these results revealed that the latter is an electron donor while the former is an electron acceptor.

Table 9. The electronic reactivity descriptors of DCNP and ADMP.

	B3LYP			CAM-B3LYP		
DCNP	**Gas**	**ACN**	**EtOH**	**Gas**	**ACN**	**EtOH**
E_{HOMO}	–7.5575	–7.3275	–7.6418	–8.9594	–8.7175	–8.7129
E_{LUMO}	–3.1525	–3.2009	–7.3232	–1.8196	–1.8591	–1.8605
I	7.5575	7.3275	7.6418	8.9594	8.7175	8.7129
A	3.1525	3.2009	7.3232	1.8196	1.8591	1.8605
η	–5.3550	–5.2642	–7.4825	–5.3895	–5.2883	–5.2867
μ	2.2025	2.0633	0.1593	3.5699	3.4292	3.4262
ω	6.5098	6.7154	175.7048	4.0683	4.0776	4.0787
ADMP						
E_{HOMO}	–6.2119	–6.4296	–6.4347	–7.6470	–7.8726	–7.8783
E_{LUMO}	–0.2762	–0.5108	–0.5170	0.3739	0.4308	0.4308
I	6.2119	6.4296	6.4347	7.6470	7.8726	7.8783
A	0.2762	0.5108	0.5170	–0.3739	–0.4308	–0.4308
η	–3.2440	–3.4702	–3.4759	–3.6366	–3.7209	–3.7238
μ	2.9678	2.9594	2.9589	4.0104	4.1517	4.1545
ω	1.7730	2.0345	2.0416	1.6488	1.6674	1.6688

- **Electronic spectra**

The calculated UV–Vis spectrum, using the CAM-B3LYP method in EtOH was used to simulate the experimental findings (**Table S1** (Supplementary data)). The calculated spectra of the PT complex predicted a broad band at 339.3 nm and oscillator strength (f) of 0.605 (**Fig. 12**). This band is assigned mainly (97 %) due to HOMO→LUMO excitation (**Fig. 13**). Both HOMO and LUMO demands are delocalized over the deprotonated DCNP π-system indicating a π→π* internal electronic transition within the proton donor moiety (DCNP). The calculated transition energy for this electronic transition band is 3.655 eV, which agrees with the experimentally observed value of 3.054 eV.

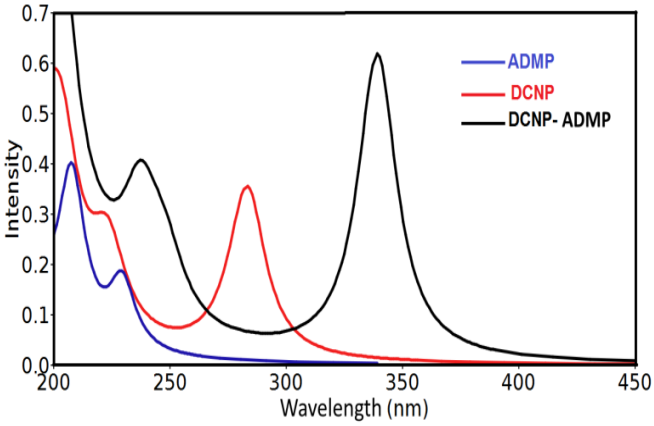

Fig. 12 The calculated electronic spectra of the studied systems in EtOH.

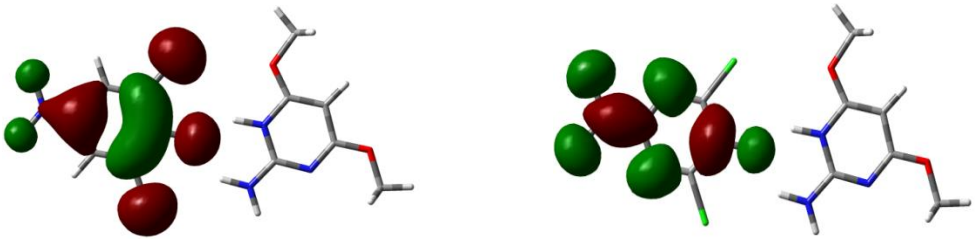

E_{HOMO}= -7.426 eV **E_{LUMO}= -1.447 eV**

Fig.13. The HOMO and LUMO demand contributed to the electronic absorption band observed in the visible region for the studied complex in EtOH calculated using CAM-B3LYP method.

- **Natural bond orbital (NBO) analysis**

The donor NBO_i-acceptor NBO_j interaction energies $E^{(2)}$ for DCNP, ADMP, and the DCNP-ADMP complex are given in **Table 10**. The electron delocalization that occurred in the DCNP-ADMP complex showed significant variations compared to the free molecules. The most apparent change is the disappearance of the LP(1)N5 to the neighboring σ* antibonding natural orbitals, which are attributed to the protonation of the pyrimidine N-atom of ADMP molecule. Moreover, the LP(1)N7→ BD*(2)C4-N5 intramolecular charge transfer is almost doubled in the [DCNP-ADMP] PT complex (96.06 kcal mol^{-1}) compared to the free molecule (47.43 kcal mol^{-1}). This could be attributed to the hydrogen bonding interaction occurring between the N-H (amino) proton of ADMP with the phenolic O-atom of the DCNP molecule. Also, it should be noted that the majority of the π→π* electron delocalization in the DCNP moiety did not occur in the [DCNP-ADMP] PT complex. In addition, the three new intramolecular charge transfer interactions LP(1)O32→BD*(1)N5-H35 /BD*(1)N7-H14 and LP(2)O32→BD*(1)N5-H35 with interaction energies of 15.34, 15.00, and 32.07 kcal mol^{-1}, respectively stabilized the hydrogen bonding interactions, which occurred in the [DCNP-ADMP] PT complex.

Table 10. The stabilization energies arise from the inter- and intra-molecular charge transfer interaction in the free DCNP, ADMP and [DCNP-ADMP] PT complex.

Donor NBO	Acceptor NBO	[DCNP-ADMP]	Free molecule
Within ADMP			
BD(1)C1-C2	BD*(1)C6-O8	6.00	5.32
BD(1)C1-C2	BD*(1)O10-C11	3.42	3.22
BD(1)C1-C6	BD*(1)C2-O10	3.50	4.22
BD(2)C1-C6	BD*(2)C1-C6	6.54	4.92
BD(2)C1-C6	BD*(2)C2-N3	32.87	36.10
BD(2)C1-C6	BD*(2)C4-N5	5.57	8.26
BD(1)C2-N3	BD*(1)C4-N7	4.18	4.01
BD(2)C2-N3	BD*(2)C1-C6	5.50	5.86
BD(2)C2-N3	BD*(2)C4-N5	43.28	35.36
BD(1)N3-C4	BD*(1)C2-O10	4.41	5.11
BD(2)C4-N5	BD*(2)C1-C6	29.00	34.59
BD(2)C4-N5	BD*(2)C2-N3	2.87	5.54
LP(1)N3	BD*(1)C1-C2	10.75	10.50
LP(1)N3	BD*(1)C2-O10	5.57	5.13
LP(1)N3	BD*(1)C4-N5	13.21	13.29
LP(1)N5	BD*(1)C1-C6	-	10.53
LP(1)N5	BD*(1)N3-C4	-	14.77
LP(1)N5	BD*(1)C4-N7	-	3.09
LP(1)N5	BD*(1)C6-O8	-	5.81
LP(1)N7	BD*(2)C4-N5	96.06	47.43
LP(1)O8	BD*(1)C1-C6	8.55	7.52
LP(2)O8	BD*(2)C1-C6	43.64	37.40
LP(1)O10	BD*(1)C2-N3	8.11	7.52
LP(2)O10	BD*(2)C2-N3	47.24	41.00
LP(2)O10			
Within DCNP			
BD(2)C23-C24	BD*(2)C1-C2		23.98
BD(2)C23-C24	BD*(2)C5 -C6		16.53
BD(2)C23-C24	BD*(2)N7 -O8		27.81
BD(2)C25-C26	BD*(2)C1-C2		14.09
BD(2)C25-C26	BD*(2)C3 -C4		23.62
BD(2)N 27-O28	BD*(2)C3-C4		4.22
BD(2)N27-O29	BD*(2)N27-O29	8.06	7.56
LP(2)O28	BD*(1)C23-N27	10.61	12.01

LP(2)O28	BD*(1)N27-O28	19.14	19.25
LP(3)O28	BD*(2)N27-O29	153.58	160.52
LP(3)Cl30	BD*(2)C24-C25	10.78	11.05
LP(1)O29	BD*(1)C23-N27	4.36	4.20
LP(1)O29	BD*(1)N27-O28	2.34	2.59
LP(2)O29	BD*(1)C23-N27	10.61	11.96
LP(2)O29	BD*(1)N27-O28	19.14	19.18
LP(3)Cl31	BD*(2)C21-C22	10.97	12.98
LP(1)O32	BD*(1)C21-C26	6.29	6.90
LP(2)O32	BD*(1)C21-C26	6.94	
	BD*(1)C25-C26	14.83	35.92
DCNP→ ADMP			
LP(1)O32	BD*(1)N5-H35	15.34	
LP(1)O32	BD*(1)N7-H14	15.00	
LP(2)O32	BD*(1)N5-H35	32.07	

Conclusion

The reaction between the proton donor, DCNP with proton acceptor, ADMP has been investigated in three different solvents and in the solid state. The formed PT complex was studied spectrophotometrically as well as theoretically. In all investigated solvents, the complex showed stable absorption after two hours and 20°C was the optimum temperature, where the absorbance presented the highest values. Job's of continuous variation and spectrophotometric titration methods confirmed the formation of a 1:1 (donor: acceptor) complex in all solvents. The K_{PT} of the complex was estimated, using modified Benesi-Hildebrand equation, where the highest value was recorded in EtOH. ADMP was effectively determined with a high degree of accuracy and precision. The solid complex was characterized by the elemental analysis, which confirmed its formation in a 1:1 ratio and was consistent across the three solvents tested. Moreover, ^{1}H NMR and FT-IR spectra confirmed the formation of hydrogen-bonded proton transfer complex. The results confirmed the contribution of both the amino group and the ring nitrogen of ADMP in hydrogen bonding with OH of DCNP. DFT studies indicated that DCNP is the electron acceptor while ADMP is the electron donor. The electron density transferred from ADMP to DCNP is 0.142 e for an isolated system and found to be less (0.083 e) in the solution. The effects of hydrogen bonding interactions and proton transfer on the electron delocalization processes in the studied system were discussed using NBO method. Also, the UV-Vis spectra were simulated using TD-DFT calculations.

Supplementary Information (SI)

The suggested mechanism of the [DCNP-ADMP] PT complex, ^{1}H NMR spectrum of [DCNP-ADMP] PT complex in DMSO-*d6*, and the lowest 50 spin-allowed excitation states of the studied proton transfer complex (**Scheme S1, Fig. S1, and Table S1)** are available.

References

1. Katritzky, A.R., Ramsden, C.A., Scriven, E.F.V. and Taylor, R.J.K.. Comprehensive heterocyclic chemistry III (Vol. 4, p. 1). Amsterdam: Elsevier, 2008.
2. Lagoja IM. Pyrimidine as constituent of natural biologically active compounds. Chemistry & Biodiversity. 2005 Jan;2(1):1-50.
3. Faizan M, Bhat SA, Alam MJ, Afroz Z, Ahmad S. Anharmonic vibrational and electronic spectral study of 2-amino-4-hydroxy-6–methylpyrimidine: A combined experimental (FTIR, FT-Raman, UV–Vis) and theoretical (DFT, MP2) approach. Journal of Molecular Structure. 2017 Nov 15;1148:89-100.
4. A Naikoo R, A Mir M, Bhat S, Tomar R, A Bhat R, A Malla M. Biological activities and synthetic approaches of dihydropyrimidinones and thiones-an updated review. Current Bioactive Compounds. 2016 Dec 1;12(4):236-50.
5. Sharma V, Chitranshi N, Agarwal AK. Significance and biological importance of pyrimidine in the microbial world. International journal of medicinal chemistry. 2014;2014.
6. Vorbrüggen H. Advances in amination of nitrogen heterocycles. InAdvances in Heterocyclic chemistry 1990 Jan 1 (Vol. 49, pp. 117-192). Academic Press.
7. Schomaker JM, Delia TJ. Arylation of halogenated pyrimidines via a Suzuki coupling reaction. The Journal of organic chemistry. 2001 Oct 19;66(21):7125-8.

8. Aparna EP, Devaky KS. Advances in the Solid-Phase Synthesis of Pyrimidine Derivatives. ACS Combinatorial Science. 2019 Jan 4;21(2):35-68.
9. Habeeb MM, Al-Attas AS, Basha MT. Spectrophotometric studies of proton transfer complexes between 2-amino-4-methoxy-6-methyl-pyrimidine and 2-amino-4, 6-dimethyl-pyrimidine with 2, 6-dichloro-4-nitrophenol in acetonitrile. Journal of Molecular Liquids. 2009 Nov 15;150(1-3):56-61.
10. Kanani MB, Patel MP. Synthesis of N-arylquinolone derivatives bearing 2-thiophenoxyquinolines and their antimicrobial evaluation. Chinese Chemical Letters. 2014 Jul 1;25(7):1073-6.
11. Yang D, Zhao F, Zheng R, Lv J. Influence of intermolecular hydrogen bonding and solvent effects on the excited-state properties of a photoactive yellow protein chromophore compound. Journal of Alloys and Compounds. 2016 Feb 25;659:82-9.
12. Zhao GJ, Han KL. Site-specific solvation of the photoexcited protochlorophyllide a in methanol: formation of the hydrogen-bonded intermediate state induced by hydrogen-bond strengthening. Biophysical journal. 2008 Jan 1;94(1):38-46.
13. Yang D, Qi R. Effects of intermolecular hydrogen bonding on the excited-state proton transfer properties of the cinnamonitrile–methanol complex. Canadian Journal of Chemistry. 2013 Mar 18;91(3):229-34.
14. Han KL, Zhao GJ. Hydrogen bonding and transfer in the excited state. John Wiley & Sons; 2011 Mar 16.
15. Alexeev YE, Kharisov BI, García TH, Garnovskii AD. Coordination motifs in modern supramolecular chemistry. Coordination Chemistry Reviews. 2010 Apr 1;254(7-8):794-831.
16. Gregoire G, Jouvet C, Dedonder C, Sobolewski AL. On the role of dissociative πσ* states in the photochemistry of protonated tryptamine and tryptophan: An ab initio study. Chemical physics. 2006 May 31;324(2-3):398-404.
17. Deechongkit S, Nguyen H, Powers ET, Dawson PE, Gruebele M, Kelly JW. Context-dependent contributions of backbone hydrogen bonding to β-sheet folding energetics. Nature. 2004 Jul;430(6995):101.
18. Dega-Szafran Z, Dutkiewicz G, Kosturkiewicz Z, Petryna M, Szafran M. Crystal and molecular structure of the 1: 1 complex of 1-piperidineacetic acid with 2, 6-dichloro-4-nitrophenol studied by X-ray diffraction and B3LYP calculation. Journal of molecular structure. 2005 May 2;741(1-3):115-20.
19. Al-Ahmary KM, Habeeb MM, Al-Solmy EA. Spectroscopic investigation on proton transfer reaction in the complex of 2-aminopyridine with 2, 6-dichloro-4-nitrophenol in different solvents. Journal of Molecular Liquids. 2011 Feb 1;158(3):161-5.
20. Al-Ahmary KM, Al-Solmy EA, Habeeb MM. Spectroscopic characterization of hydrogen-bonded proton transfer complex between 4-aminopyridine with 2, 6-dichloro-4-nitrophenol in different solvents and solid state. Spectrochimica Acta Part A: Molecular and Biomolecular Spectroscopy. 2014 May 21;126:260-9.
21. Al-Ahmary KM, Habeeb MM, Al-Obidan AH. Spectrophotometric study on the proton transfer reaction between 2-amino-4-methylpyridine with 2, 6-dichloro-4-nitrophenol in methanol, acetonitrile and the binary mixture 50% methanol+ 50% acetonitrile. Spectrochimica Acta Part A: Molecular and Biomolecular Spectroscopy. 2016 Feb 5;154:135-44.
22. Al-Ahmary KM, Soliman SM, Habeeb MM, Al-Obidan AH. Spectral analysis and DFT computations of the hydrogen bonded complex between 2, 6-diaminopyridine with 2, 6-dichloro-4-nitrophenol in different solvents. Journal of Molecular Structure. 2017 Sep 5;1143:31-41.
23. Dega-Szafran Z, Komasa A, Olejniczak A, Katrusiak A, Szafran M. Spectroscopic and theoretical studies of the H-bonded complex of quinuclidine with 2, 6-dichloro-4-nitrophenol. Vibrational Spectroscopy. 2017 Nov 1;93:29-35.
24. Dega-Szafran Z, Bartoszak-Adamska E, Baranowska A, Komasa A, Szafran M. Cooperative hydrogen bond between piperidine-ethanol and 2, 6-dichloro-4-nitrophenol. Journal of Molecular Structure. 2019 May 15;1184:468-78.
25. Frisch MJ, Trucks GW, Schlegel HB, Scuseria GE, Robb MA, Cheeseman JR, Scalmani G, Barone V, Mennucci B, Petersson GA, Nakatsuji H. Gaussian 09, Rev. D. 01, Gaussian. Inc., Wallingford, CT. 2009.
26. GaussView V. 4.1, R. Dennington II, T. Keith, and J. Millam, Semichem. Inc., Shawnee Mission, KS. 2007.
27. Zhurko GA, Zhurko DA. Chemcraft: Lite Version Build 08 (Freeware).

28. Version NB, Glendening ED, Reed AE, Carpenter JE, Weinhold F. NBO Version 3.1, CI,1998.
29. Reed AE, Curtiss LA, Weinhold F. Intermolecular interactions from a natural bond orbital, donor-acceptor viewpoint. Chemical Reviews. 1988 Sep 1;88(6):899-926.
30. Cossi M, Scalmani G, Rega N, Barone V. New developments in the polarizable continuum model for quantum mechanical and classical calculations on molecules in solution. The Journal of Chemical Physics. 2002 Jul 1;117(1):43-54.
31. Dega-Szafran Z, Dulewicz E, Szafran M. Spectroscopic studies of N-methylpiperidine betaine complexes with phenols. Journal of molecular structure. 2004 Oct 18;704(1-3):155-61.
32. Job P. Formation and stability of inorganic complexes in solution. 1928.
33. Skoog, D.A.. Principles of Instrumental Analysis, 3rd. Edn., HRW International Edition, Philadelphia, 1985; 728-730.
34. Benesi HA, Hildebrand JH. A spectrophotometric investigation of the interaction of iodine with aromatic hydrocarbons. Journal of the American Chemical Society. 1949 Aug;71(8):2703-7.
35. Airinei A, Homocianu MI, Dorohoi DO. Changes induced by solvent polarity in electronic absorption spectra of some azo disperse dyes. Journal of Molecular Liquids. 2010 Nov 15;157(1):13-7.
36. Voigt EM, Reid C. Ionization potentials of substituted benzenes and their charge-transfer spectra with tetracyanoethylene. Journal of the American Chemical Society. 1964 Oct;86(19):3930-4.
37. Lever A.B.P., Inorganic Electronic Spectroscopy 2nd (Ed.) (Amsterdam: Elsevier). 1985.
38. Martin AN, Swarbrick J, Cammarata A. Physical pharmacy, 3rd. Lee and Febiger, Philadelphia. 1983;344.
39. Miller, J.C., Miller, J.N. Statistics for Analytical Chemistry, 2nd (Ed.) (England: Ellis Horwood Limited). 1988.
40. Foresman, J.B., Frisch, A.E., Exploring Chemistry with Electronic Structure Methods, 2nd edn. Gaussian Inc., Pittsburgh, PA. Search PubMed, 1996.
41. Chang R. Chemistry seventh (Ed.) (New York: McGraw-Hill), 2001.
42. Kosar B, Albayrak C. Spectroscopic investigations and quantum chemical computational study of (E)-4-methoxy-2-[(p-tolylimino) methyl] phenol. Spectrochimica Acta Part A: Molecular and Biomolecular Spectroscopy. 2011 Jan 1;78(1):160-7.
43. Koopmans T. Ordering of wave functions and eigenenergies to the individual electrons of an atom. Physica. 1933;1:104-13.
44. Parr RG, Yang W. Density-Functional Theory of Atoms and Molecules, Oxford Univ. Press, New York. 1989.
45. Parr RG. v. Szentpály, L.; Liu, S. J. Am. Chem. Soc. 1999;121:1922.
46. Scott AP, Radom L. Harmonic vibrational frequencies: an evaluation of Hartree− Fock, Møller− Plesset, quadratic configuration interaction, density functional theory, and semiempirical scale factors. The Journal of Physical Chemistry. 1996 Oct 10;100(41):16502-13.